On the Physics of Towed Streamer Controlled Source Electromagnetics in Shallow Water in the Presence of Transverse Anisotropy

*Alan D Chave** (*Woods Hole Oceanographic Institution, Woods Hole, MA 02543, USA*)
Johan Mattsson (*PGS, S-164-46 Kista, Stockholm, Sweden*)
Mark E Everett (*Texas A&M University, College Station, TX 77845, USA*)

Summary

In recent years, marine controlled source electromagnetics (CSEM) has found increasing use in hydrocarbon exploration due to its ability to detect thin resistive zones beneath the seafloor. It is the purpose of this paper to evaluate the effect of an electrically-thin ocean on the physics of CSEM using the towed streamer in-line configuration through examination of the electric field and the time-averaged energy flow depicted by the real part of the complex Poynting vector, and for an isotropic and transversely anisotropic sedimentary sequence. The observable electric field following excitation by a horizontal electric dipole (HED) source can be understood through the energy flow within the entire structure caused by the competing influences of guided energy flow in the reservoir layer and the air interaction. The influence of transverse anisotropy in a sedimentary sequence is to enhance the effect of guided energy flow as compared to an isotropic structure, yielding a response that is analogous to that in deeper water for an isotropic medium.

Introduction

Pioneering measurements by Charles Cox showed that the natural electric field background level at frequencies in the vicinity of 1 Hz in the deep ocean is extremely weak, suggesting that the fields induced within Earth by a near-seafloor artificial source could be detected at large (many km) offsets. This led to the development of a practical geophysical exploration method based on seabed-to-seabed propagation of low frequency EM fields from a HED source. However, in shallow water, inductive coupling of the sea surface with the entire resistivity structure (hereafter called the air interaction) has a profound effect on the measured electromagnetic field. This was characterized in detail by Chave et al. (2017) for the 1D isotropic case through examination of the in-line seafloor electric field from a near bottom source (hereafter the seafloor configuration) and Poynting vector throughout the structure. It is the purpose of this paper to extend that study to a shallow towed streamer configuration that includes consideration of transverse anisotropy in the underburden and overburden.

Theory

Oil reservoirs are thin, geologically-complex structures of variable hydrocarbon saturation and finite lateral extent located within sedimentary sequences, overlain by bathymetric variations and underlain by crystalline basement rock. Despite the gross oversimplification of the actual geology of a petroleum trap, it has long proved instructive to analyze the CSEM response of a 1D model in which the oil reservoir is a thin resistive layer of infinite lateral extent buried within a plane-layered, isotropic or transversely anisotropic halfspace. The canonical reservoir model used in this paper consists of a water layer of variable thickness underlain by a 1000 m thick, 2 Ω-m overburden, a 100 m thick, 20 Ω-m reservoir layer and a 2 Ω-m underburden halfspace. Both an anisotropic and transversely anisotropic (6 Ω-m vertical resistivity) overburden and underburden will be considered. A point HED of unit source moment is located 10 m below the sea surface at the origin, and in-line electric field receivers are placed at the smaller of 100 m or half of the water depth.

The physics of marine CSEM is that of diffusion driven by a periodic source, and standard frequency domain solutions are extant (Chave, 2009). Because of the diffusion physics, neither rays nor wave reflection/refraction can exist, and hence examination of the energy flux throughout the structure is the best tool to understand the EM field behavior. Poynting's Theorem in the diffusion limit and for a time harmonic source holds that the real part of the time averaged Poynting vector represents the time averaged energy flux into a volume of material that is balanced by thermodynamically-irreversible Joule heating.

Results

Figure 1 shows the Poynting vector as a function of offset and depth for a water layer thickness of 300 m at 0.1 Hz for the isotropic subsurface model. The skin depth in seawater (overburden) is 890 m (2.3 km), so the receivers are ~0.1 skin depth below the sea surface and ~0.7 skin depth above the reservoir, and hence the air interaction should dominate excitation of the reservoir at large source-receiver offsets. At offsets under ~9000 m, guided energy flow within the reservoir layer is nearly horizontal and leaks into the overburden and underburden, decreasing monotonically with range. For a given range, the largest Poynting vector magnitude is observed within the reservoir layer out to

~8000 m. The energy flux within the water layer is downward away from the sea surface, diagnostic of the effect of the air interaction. Figure 1 is nearly identical to the Poynting vector in the seafloor configuration, with the flux transitions (i.e., the abrupt shift of the direction of energy flow from predominantly outward/upward to predominantly downward) occurring about 1 km closer to the source.

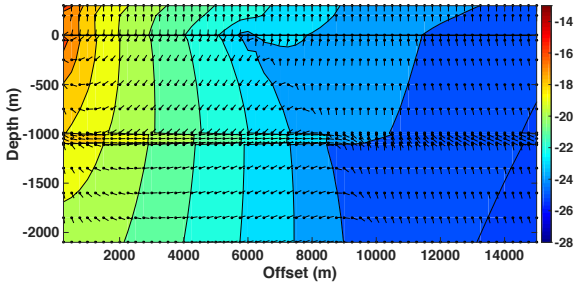

Figure 1. Contours of the logarithm (base 10) of the magnitude of the Poynting vector as a function of source-receiver offset and depth for the isotropic canonical model. The water depth is 300 m, the source frequency is 0.1 Hz and the configuration is towed streamer. The seafloor is depicted by a solid horizontal black line. The Poynting vector plot also shows the direction of energy flow at each of the small circles throughout the structure. The arrow orientations have been adjusted for the different horizontal and vertical scales.

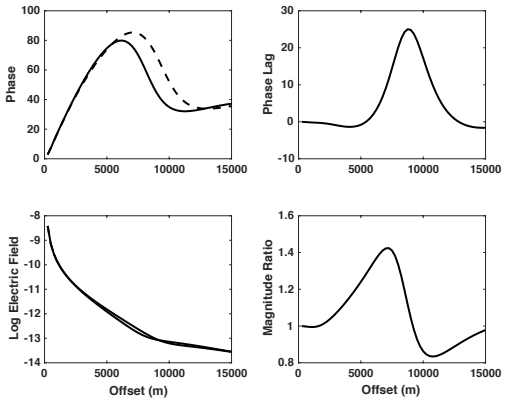

Figure 2. The in-line electric field at 100 m water depth as a function of offset in the towed streamer configuration. The water depth is 300 m and the source frequency is 0.1 Hz. From the upper left and proceeding counter-clockwise, the panels show the phase of the reservoir and halfspace responses, the base 10 logarithm of the magnitude of the reservoir and halfspace responses, the magnitude ratio of the reservoir to the halfspace response and the phase lag between the reservoir and halfspace responses. The dashed line is the reservoir result while the solid line is the halfspace result.

Figure 2 shows the in-line electric field amplitude and phase at the towed receivers corresponding to Figure 1 for both the reservoir and halfspace models. The phase convention is such that a lower phase for the reservoir model, or negative phase lag, represents a faster response compared to the halfspace one, while a normalized electric field larger than unity represents a stronger reservoir model response than that to a halfspace. The response to the reservoir is stronger and very slightly faster from ~2-6 km offset, then stronger and slower to ~9 km and finally weaker and slower. The transitions in Figure 2 systematically occur at 1-2 km shorter offsets as compared to a seafloor configuration model.

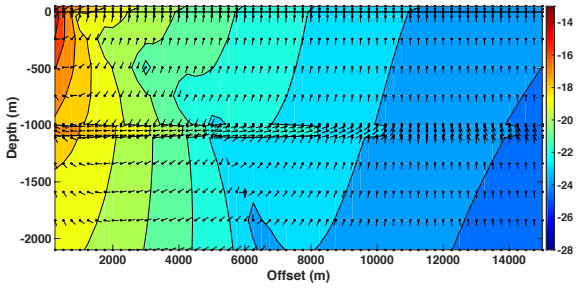

Figure 3. Contours of the logarithm (base 10) of the magnitude of the Poynting vector as a function of source-receiver offset and depth for the isotropic canonical model. The water depth is 50 m, the source frequency is 0.1 Hz and the configuration is towed streamer. See Figure 1 caption for details.

Figure 3 shows the Poynting vector for 50 m water depth and a 0.1 Hz source for the isotropic subsurface model. The receivers are ~0.03 skin depth beneath the sea surface and ~0.5 skin depths above the reservoir. The Poynting vector plot is qualitatively similar to that in Figure 1, except that changes in energy flow direction occur at smaller offsets throughout the structure and the direction of guided energy flux in the reservoir layer is fully reversed (i.e., directed toward the source) at offsets of ~5-10 km, gradually rotating downward and then slightly outward at longer distances. Associated with the energy flux confluence at ~5 km within the reservoir layer, the flow direction in the underburden abruptly shifts from upward, outward to downward, inward. A minimum in the Poynting vector amplitude is also observed extending from near the source downward to the reservoir layer at ~5 km and then further into the underburden. The locus of the minimum represents a shift from dominance by the response to the dipole source (including galvanic reservoir excitation) to dominance by the air interaction. The outward energy flux tongue in the reservoir layer decreases in length up to ~5 km, then increases over the interval exhibiting reversed energy flux and ultimately gets smaller at the longest source-receiver offsets.

Figure 4 shows the seafloor electric field corresponding to the shallow water model of Figure 3. The amplitude ratio is greater than unity over ~2-9 km, and becomes very weakly

negative beyond that point out to ~12 km. The phase for the reservoir model lags that for a halfspace over ~5-12 km, and has a weak lead at shorter offsets. Consequently, the reservoir response is stronger and slightly faster at short (~0-5 km) offsets, substantially stronger and slower at intermediate (~5-9 km) offsets, then becomes weaker and slower at large offsets. Overall, the seafloor electric field is an attenuated version of the 300 m water depth result in Figure 2, with the additional influence of the flux reversal in the reservoir layer.

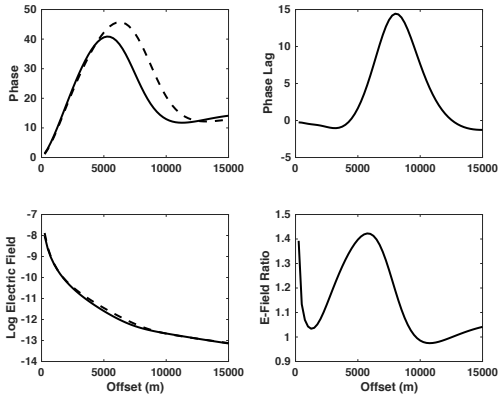

Figure 4. The in-line electric field at 25 m water depth as a function of offset in the towed streamer configuration. The water depth is 50 m and the source frequency is 0.1 Hz. See Figure 2 caption for details.

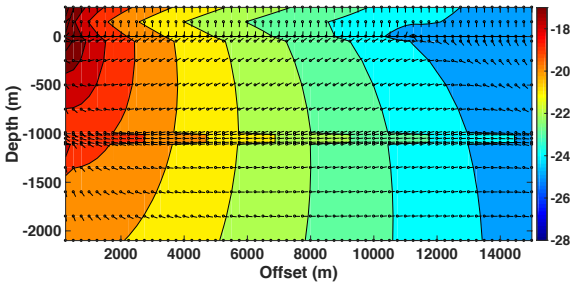

Figure 5. Contours of the logarithm (base 10) of the magnitude of the Poynting vector as a function of source-receiver offset and depth for the transversely anisotropic canonical model. The water depth is 300 m, the source frequency is 0.1 Hz and the configuration is towed streamer. See Figure 1 caption for details.

Figure 5 shows the Poynting vector for 300 m water depth at 0.1 Hz for the transversely anisotropic model. The energy flux in this model is quite different from that in Figures 1 and 3, as the outward-directed guided energy flow in the reservoir layer extends to much longer offsets, and in fact resembles a deep water isotropic model. The energy flux in the overburden is upward, outward from the reservoir layer to ~12 km offset, beyond which it abruptly shifts to downward, outward

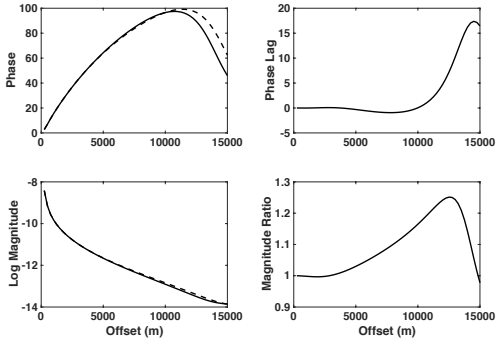

Figure 6. The in-line electric field at 100 m water depth as a function of offset for the transversely anisotropic model. The water depth is 300 m and the source frequency is 0.1 Hz. See Figure 2 caption for details.

Figure 6 shows the in-line electric field amplitude and phase for the 300 m water depth transversely anisotropic model, where the halfspace model used for comparison is transversely anisotropic. Figure 6 resembles Figure 1 pushed substantially to longer offsets. The right panels show a stronger and weakly faster response from ~2-10 km and a stronger and slower one beyond that point.

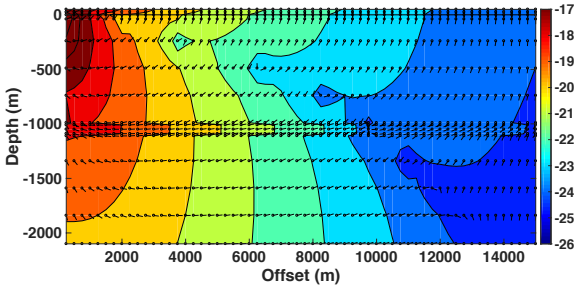

Figure 7. Contours of the logarithm (base 10) of the magnitude of the Poynting vector as a function of source-receiver offset and depth for the transversely anisotropic canonical model. The water depth is 50 m, the source frequency is 0.1 Hz and the configuration is towed streamer. See Figure 1 caption for details.

Figure 7 shows the Poynting vector for 50 m water depth at 0.1 Hz for the transversely anisotropic model. The energy flux resembles that seen in Figure 3, but with the major transition in flux direction from outward to inward within the reservoir layer occurring at roughly twice the offset. The air interaction is apparent within the overburden as a shift in flux direction from upward, outward to downward, inward that transitions at ~2 km offset at the seafloor to ~10 km at the top of the reservoir layer.

Figure 8 shows the in-line electric field for the 50 m water depth transversely anisotropic model of Figure 7. As for the 300 m case, it resembles the isotropic result in Figure 4

pushed substantially to larger offsets. The reservoir model electric field is initially stronger and slightly faster, then transitions to stronger and slower beyond ~10 km offset.

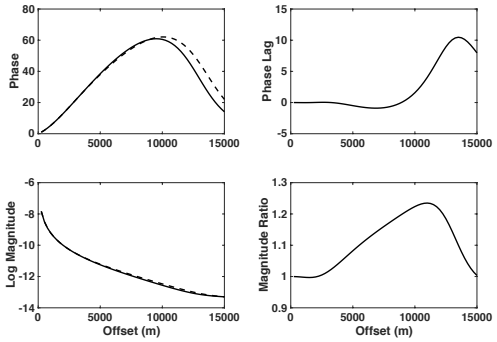

Figure 8. The in-line electric field at 25 m water depth as a function of offset for the transversely anisotropic model. The water depth is 50 m and the source frequency is 0.1 Hz. See Figure 2 caption for details.

Discussion

The Poynting vector results in Figures 1, 3, 5 and 7 reflect the competing and coupled effects of guided energy flow within the reservoir layer and the air interaction. When the ocean is electrically thicker (Figures 1 and 5), the latter does not dominate except at the longest offsets. Guided energy flow is predominant at short ranges and the air interaction is larger at long ranges, yielding a sharp transition zone that moves outward from the water layer through the overburden and into the underburden. For an ocean that is electrically thinner (Figures 3 and 5), the transition zone begins at a much shorter offset in the water layer, and the air interaction is of an appropriate polarization, and has sufficient strength at the reservoir layer, to reverse the time-averaged energy flux direction. The energy flux behavior is manifest in the key observable, the towed streamer in-line electric field, and determines whether it is stronger/weaker and faster/slower relative to the halfspace response. Chave et al. (2017) provide a physical explanation for the reservoir layer flux reversal in terms of coupling of the fundamental inductive and galvanic modes in the second order Poynting vector.

The effect of transverse anisotropy is superimposed on this simple model linking the Poynting vector and the nature of the electric field observable. The 3:1 transverse anisotropy used in this paper is a typical value for marine sedimentary sequences, and values of over 10:1 have been observed in the Barents Sea (Ellis et al., 2015). Transverse anisotropy where the vertical resistivity is larger than the horizontal resistivity has the effect of enhancing the influence of guided energy flow within the reservoir layer as compared to the air interaction. It is well known (Chave, 2009) that guided energy flow within a reservoir layer is a purely galvanic mode phenomenon, while the air interaction is due to the inductive mode. As the vertical resistivity in the overburden increases, attenuation of the galvanic mode decreases and hence excitation of the reservoir layer is enhanced, producing a higher horizontal energy flux. However, the air interaction is insensitive to the vertical resistivity, and hence its contribution is unchanged for a fixed horizontal resistivity. This results in a shift of the transition to vertical energy flux to longer offsets as compared to an isotropic model, as seen by comparing Figures 2 and 4 to Figures 6 and 8.

It has long been known that continental shelf sedimentary formations typically display transversely anisotropic electrical conductivity, and it was believed that measurements over a wide range of source-receiver azimuths would be needed to resolve both the anisotropy and the reservoir structure, with the in-line orientation primarily sensitive to the vertical conductivity and the broadside one sensitive to the horizontal conductivity. This conventional wisdom appears to militate against using the strictly in-line geometry discussed in this paper. However, a strong air interaction that is manifest as vertically-directed energy flux in the overburden (corresponding to a horizontally polarized electric field) enables the detection of both anisotropy and a reservoir layer with only the in-line geometry in shallow water provided measurements are made over a wide enough range of offsets and frequencies. By contrast, in deep water where the air interaction is weak, measurements over a wide range of source-receiver azimuths are required to resolve anisotropy. The examples presented in this paper are at the low end of the useful frequency range, and emphasize guided energy flow over the air interaction. However, by raising the frequency by 1-2 orders of magnitude, the air interaction will dominate at offsets within the practical dimensions of a towed streamer ($\lesssim$ 10 km).

Conclusions

This paper has compared the energy flow throughout a subsurface structure containing a resistive reservoir layer to the electric field measured by a towed CSEM streamer. The result can be understood by analyzing the competing influences of guided energy flow in the reservoir layer and the air interaction. When the vertical resistivity of a sedimentary sequence is higher than a given horizontal resistivity, guided energy flow is enhanced while the air interaction is fixed, so that the stronger and faster electric field associated with it extends to longer ranges as compared to the response for an isotropic structure.

EDITED REFERENCES

Note: This reference list is a copyedited version of the reference list submitted by the author. Reference lists for the 2017 SEG Technical Program Expanded Abstracts have been copyedited so that references provided with the online metadata for each paper will achieve a high degree of linking to cited sources that appear on the Web.

REFERENCES

Chave, A. D., 2009, On the electromagnetic fields produced by marine frequency domain controlled sources: *Geophysical Journal International*, *179*, 1429–1457, http://doi.org/10.1111/j.1365-246X.2009.04367.x.

Chave, A. D., M. E. Everett, J. Mattsson, J. Boon, and J. Midgely, 2017, On the physics of frequency domain controlled source electromagnetics in shallow water, 1: isotropic conductivity: *Geophysical Journal International*, *208*, 1026–1042, https://doi.org/10.1093/gji/ggw435.

Ellis, M., L. MacGregor, R. Ackermann, P. Newton, R. Keirstad, A. Rusic, S. Bouchara, A. G. Alvarez, and H.-W. Tseng, 2015, Electrical anisotropy drivers in the Snøhvit region of the Barents Sea: 85th Annual International Meeting, SEG, Expanded Abstracts, 3244–3248, https://doi.org/10.1190/segam2015-5919757.1.